ACKNOWLEDGMENTS

The authors wish to thank the Morton Salt Company for providing hospitality and facilities at their Fairport Harbor Mine, the Republic Steel Corporation for their gift of the shielding material, A. A. Hruschka for his contribution to the design and fabrication of the detectors, Professor T. L. Jenkins for valuable discussions, Mrs. C. C. Giamati for assistance in data reduction and film reading, and W. R. Kropp for help in taking data at Case Institute.

PHYSICAL REVIEW VOLUME 126, NUMBER 6 JUNE 15, 1962

$\pi^-+p\rightarrow\pi^0+n$ Charge Exchange Cross Sections at 20.7 and 31.0 Mev

K. MIYAKE,* K. F. KINSEY, AND D. E. KNAPP†
The University of Rochester, Rochester, New York

(Received November 21, 1961)

A measurement has been made of the differential and total cross sections at 31.0 Mev and the total cross section at 20.7 Mev for the reaction $\pi^-+p\rightarrow\pi^0+n$. A thin-walled liquid hydrogen target was used. The gamma telescopes used a Čerenkov counter to identify the conversion electrons and a thin-lead converter to avoid complications from cascade processes. The angular distribution in mb/sr at 31.0 Mev is: $d\sigma/d\Omega=(1.00\pm0.02)[(0.51\pm0.04)-(0.61\pm0.11)P_1(\cos\theta)+(0.12\pm0.36)P_2(\cos\theta)]$. The total cross sections at 31.0 and 20.7 Mev are 6.5 ± 0.5 and 5.4 ± 0.4 mb, respectively. The data are also analyzed in terms of the phase shifts α_{ij}. Assuming that the S-wave phase shifts extrapolate to zero pion energy as $\alpha_i=a_i\eta$, where η is the pion momentum in the c.m. system in units of $m_\pi c$, the quantity $(a_1-a_3)=0.27\pm0.02$. This agrees with Hamilton and Woolcock's prediction from photoproduction and the Panofsky ratio $(a_1-a_3)=0.245\pm0.01$. There are theoretical and experimental grounds for a nonlinear behavior of α_3 and α_1, which should improve the agreement.

I. INTRODUCTION

THE pion-proton interaction has been studied extensively since the advent of reasonably intense pion beams. At low pion energies (below $\sim$200 Mev), the predominant features of the scattering have been satisfactorily explained in terms of a resonance in the $T=\frac{3}{2}$, $J=\frac{3}{2}$ state at $\sim$170 Mev. However, because of the dominance of this resonance, the smaller phase shifts have been more difficult to measure and there still remain problems concerning their behavior, especially at low energy. In particular, the quantity $(\alpha_1-\alpha_3)/\eta$ (where α_i are the S-wave phase shifts for the two isotopic spin states and η is the center-of-mass pion momentum in units of $m_\pi c$) can be calculated, in the limit of zero energy, from low energy scattering data and independently, from the Panofsky ratio and pion photoproduction data. There has been some discrepancy between the results of these two ways of calculating this quantity.

The charge exchange reaction, $\pi^-+p\rightarrow\pi^0+n$, provides a sensitive determination of this quantity, and furthermore, the Coulomb corrections to the phase shifts, important for the elastic scattering at these energies, are not present. This reaction has been measured at this laboratory by Spry[1] and by Roberts and Tinlot.[2,3] The experimental uncertainties in these measurements are considerably greater than for the presently available data on the elastic scattering processes near 30 Mev.[4–7] In this paper we report a measurement of the total and differential cross sections at 31 Mev and a total cross section measurement at 20.7 Mev for the charge exchange reaction. There is now a complete set of data of comparable accuracy for all of the observable pion-proton interactions at 31 Mev. The value of $(\alpha_1-\alpha_3)/\eta$ obtained is shown to be in reasonable agreement with the prediction from the Panofsky ratio, etc.

The technique of the present experiment differs from the previous work[1–3] in three respects:

(1) A thin lead converter (about 0.3 radiation lengths) was used to avoid complications arising from cascade processes.

(2) A Čerenkov counter was used to detect and identify the conversion electrons. This eliminated a great deal of the background.

(3) The pions were scattered by a thin-walled liquid-hydrogen target. These improvements contribute to the higher accuracy of the experiment and should introduce a different set of possible systematic errors.

* Present address: University of Kyoto, Kyoto, Japan.
† Present address: Douglas Aircraft Corporation, Santa Monica, California.
[1] W. Spry, Phys. Rev. **95**, 1295 (1954).
[2] A. Roberts and J. Tinlot, Phys. Rev. **90**, 951 (1953).
[3] J. Tinlot and A. Roberts, Phys. Rev. **94**, 137 (1954).
[4] W. B. Johnson and M. Camac, Bull. Am. Phys. Soc. **3**, 197 (1958).
[5] S. W. Barnes, B. Rose, G. Giacomelli, J. Ring, K. Miyake, and K. Kinsey, Phys. Rev. **117**, 226 (1960).
[6] S. W. Barnes, H. Winick, K. Miyake, and K. Kinsey, Phys. Rev. **117**, 238 (1960).
[7] G. Giacomelli, Phys. Rev. **117**, 250 (1960).

II. EXPERIMENTAL FORMULAS

The differential scattering cross sections for the pion-proton interactions up to an energy of around 200 Mev, can be expressed satisfactorily in terms of the S and P partial waves. Thus, we may expand the cross section either in terms of the six S and P phase shifts or equivalently, in terms of the first three Legendre polynomials:

$$d\sigma(\theta)/d\Omega = A_0 + A_1 P_1(\cos\theta) + A_2 P_2(\cos\theta). \quad (1)$$

The total cross section, obtained by integrating over θ, is given by

$$\sigma = 4\pi A_0. \quad (2)$$

If we assume that the decay of the π^0 is isotropic in its rest frame, the transformation into the laboratory system yields the following expression for the angular and energy distribution of the decay gamma rays:

$$I(\theta,k) = Q + R/k + S/k^2, \quad (3)$$

where

$$Q = \frac{2}{\gamma_0\beta_0 m\gamma(1-\beta\cos\theta)}\left\{A_0 + A_1\frac{\cos\theta-\beta}{1-\beta\cos\theta}\frac{1}{\beta_0} + \frac{A_2}{4}\left[3\left(\frac{\cos\theta-\beta}{1-\beta\cos\theta}\right)^2 - 1\right]\left(\frac{3}{\beta_0^2} - 1\right)\right\},$$

$$R = \frac{1}{[\beta_0\gamma_0\gamma(1-\beta\cos\theta)]^2}\left\{A_1\frac{\cos\theta-\beta}{1-\beta\cos\theta} + A_2\frac{3}{2\beta_0}\left[3\left(\frac{\cos\theta-\beta}{1-\beta\cos\theta}\right)^2 - 1\right]\right\}, \quad (4)$$

$$S = \frac{3mA_2}{[2\gamma_0\beta_0\gamma(1-\beta\cos\theta)]^3}\left[3\left(\frac{\cos\theta-\beta}{1-\beta\cos\theta}\right)^2 - 1\right],$$

and β_0 is the velocity of the π^0 in the center-of-mass system, $\gamma_0 = (1-\beta_0^2)^{-\frac{1}{2}}$, β is the velocity of the center-of-mass system, $\gamma = (1-\beta^2)^{-\frac{1}{2}}$, m is the mass of the π^0, θ is the direction of the decay gamma ray in the laboratory system, and k is the energy of the gamma in the laboratory system. A_0, A_1, and A_2 are the coefficients of Eq. (1) in the center-of-mass system.

Using a γ-ray detector with a detection efficiency $F(k)$, the following counting rate n can be measured:

$$n = \int\int\int I(\theta,k)F(k)n_p n_\pi d\Omega dV dk, \quad (5)$$

where n_p is the number of protons per unit volume, n_π is the number of pions incident on unit area per sec, V is the target volume, and Ω is the solid angle subtended by the gamma detector.

If a lead gamma converter is used that is sufficiently thin so that shower processes are not important, the function $F(k)$ can be closely approximated by

$$F(k) = t(\theta,\phi)\, p(1+r\ln k), \quad (6)$$

where $t(\theta,\phi)$ is the converter thickness seen by the gamma ray, and r and p are constants determined from the gamma ray absorption coefficient of lead. Using this approximation, the integration over the gamma energy k can be done, giving

$$I_F(\theta) = \int I(\theta,k)p(1+r\ln k)dk = [H(k_{\max}) - H(k_{\min})], \quad (7)$$

where

$$H(k) = p[Qk + R\ln k - S/k] + pr[Q(k\ln k - k) + \tfrac{1}{2}R(\ln k)^2 - S(\ln k + 1)/k],$$
$$k_{\min} = \frac{m\gamma_0(1-\beta_0)}{2\gamma(1+\beta\cos\theta)}; \quad k_{\max} = \frac{m\gamma_0(1+\beta_0)}{2\gamma(1-\beta\cos\theta)}. \quad (8)$$

If we define the "angular acceptance function"

$$B(\theta) = \frac{\int\int\int\int t(\theta,\phi)n_\pi(x,y)\sin\theta d\phi dx dy dz}{\int\int n_\pi(x,y)dx dy}, \quad (9)$$

where $n_\pi(x,y)$ is the beam intensity distribution over the area of the target, then the measured number of events N for N_π incident pions is

$$N = N_\pi n_p \int I_F(\theta)B(\theta)d\theta. \quad (10)$$

The quantity $B(\theta)$ is a geometrical function, depending only on the dimensions and position of the detector and target, and is weighted by the pion intensity distribution.

The phase shifts from low-energy elastic scattering predict a π^0 differential cross section sharply peaked in the backward direction. More quantitatively $A_0 \approx A_1 \gg A_2$. The gamma-ray distribution will have a similar shape, but much less strongly peaked. At 30 Mev, the kinematics are such that the two higher coefficients can be determined by measuring the angular distribution of the gamma rays; at 20 Mev the correlation between the π^0 distribution and the γ distribution is so weak that this is not practical. However, for this reason it follows that a measurement with a telescope centered at or near 90° should determine the total cross section without introducing excessive error due to the uncertainty in A_1 and A_2. The uncertainty in the total cross section due to A_1 and A_2 can be estimated from the results at 31 Mev.

The gamma-ray distribution at 31 Mev was measured with a telescope having a narrow angular acceptance

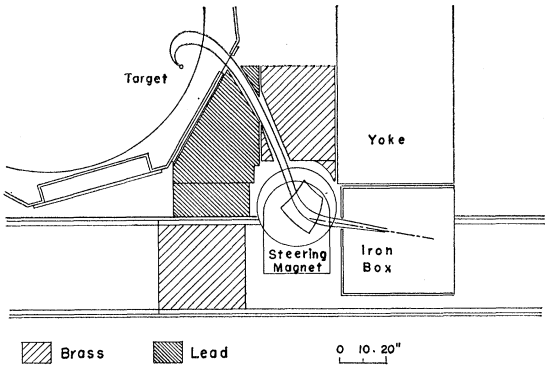

FIG. 1. General layout of cyclotron and pion beam.

and as high an efficiency as possible. As the efficiency of this telescope could not be easily measured, the angular distribution was normalized by a telescope with a large angular acceptance for which the efficiency could be accurately calculated.

A Čerenkov counter was used in the scattering telescope to identify the conversion electrons. Water was chosen as the radiating medium for two reasons: All particles, with the exception of electrons, produced by this cyclotron have velocities that are too small to radiate in water. Water also has a relatively low Z, and thereby a low conversion efficiency for the room background gamma rays, and so tends to lessen their contribution to the background counting rate.

III. EXPERIMENTAL ARRANGEMENT

A. Layout

The layout of the cyclotron and the experimental setup are shown in Fig. 1. Figure 2 is a plan view of the scattering apparatus showing two of the scattering telescopes in position. The third telescope is shown in the inset.

B. Pion Beams

The pion beam used in this experiment is produced by the 240-Mev internal proton beam of the 130-in. synchrocyclotron striking an aluminum target. The pions emerge through a thin window in the vacuum tank and travel in a channel through 3 ft of brass shielding. The beam is then deflected about 60 deg and brought to a focus by a steering magnet. The divergence of the beam was limited to approximately 4° by lead jaws on either side of the exit of the steering magnet. To reduce the cyclotron fringe magnetic field to acceptable values, the scattering apparatus was put inside a large box made of 1-in. steel plate. For the 20-Mev measurements the energy of the pion beam was reduced by placing a $\frac{5}{8}$-in. polyethylene degrader at the entrance port of the magnetic shield box.

The incident pion beam was defined by two rectangular plastic scintillation counters (referred to as No. 1 and No. 2). At normal cyclotron beam, this telescope counted $(3\text{–}4)\times10^4$ pions/min at 31 Mev. Scattering by the degrader reduced the 20-Mev beam intensity to about half this value.

The energy of the pion beams, the energy spread, and the muon and electron contaminations were measured by determining the range in copper. Although the incident beam from the cyclotron consists of about 40% electrons, it was possible to use the good pulse height resolution of counters No. 1 and No. 2 to reject all but a small fraction of the electrons. Figures 3 and 4 show typical range curves at 20 and 31 Mev, showing clearly

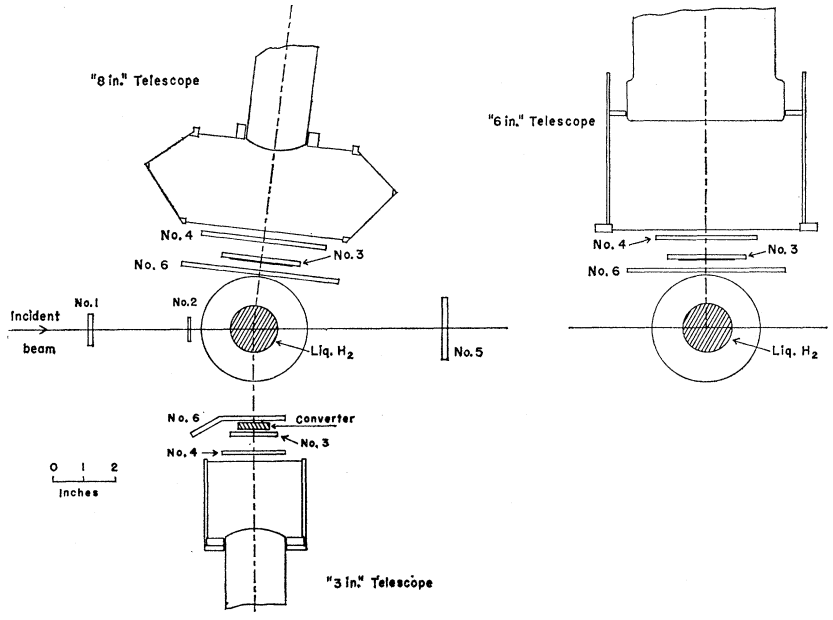

FIG. 2. Plan view of counter telescopes.

the muon and electron contaminations. The total unrejected contamination amounted to (10.3±1.5)% at 31 Mev; (9.0±1.1)% at 20 Mev.

The pion beam intensity distribution at the position of the hydrogen target was measured by a $\frac{1}{8}$-in. cube of plastic scintillator. This counter was traversed across the beam at various heights. The beam at 20 Mev was slightly more diffuse due to the degrader, but at both energies 100% of the beam (to 0.5% accuracy) passed through the target. A 1% change in the steering magnet current caused the beam center to shift about $\frac{1}{16}$ in. During the experiment this current was maintained constant to within 0.2%. No change in beam distribution was observed between traverses taken before and after the runs, within the accuracy of the traverse counter setting, estimated at $\frac{1}{32}$ in.

From the intensity distributions and the range curves, the mean pion interaction energy in the hydrogen target was calculated to be 31.0±1.7 and 20.7±2.0 Mev. The energy spread given is due partly to the different thicknesses of hydrogen traversed at different positions across the beam.

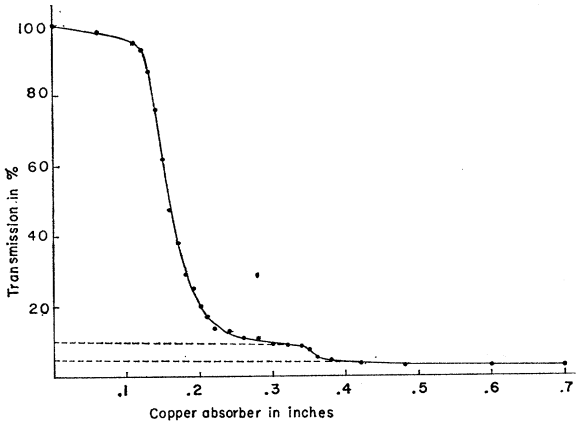

FIG. 3. Typical range curve at 20 Mev.

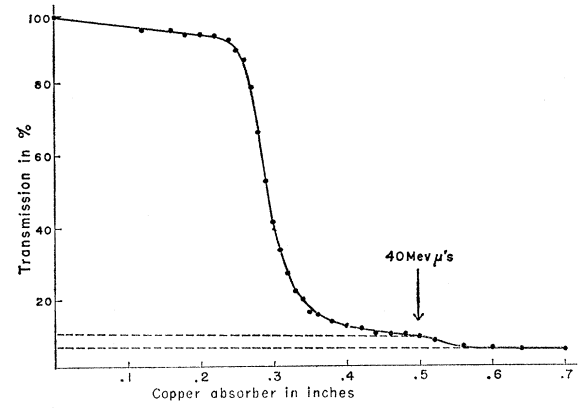

FIG. 4. Typical range curve at 31 Mev.

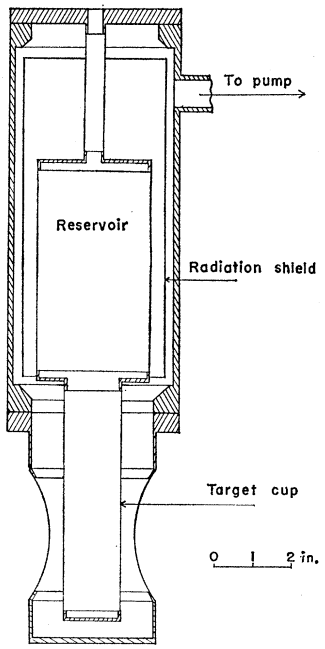

FIG. 5. Liquid-hydrogen target.

C. Liquid-Hydrogen Target

A vacuum-insulated target (Fig. 5) with a reservoir capacity of about 0.8 liter was used. The target cup was a cylinder $1\frac{1}{2}$ in. in diameter and 4 in. high. It was formed of 0.002-in. Mylar film cemented to the top and bottom flanges and along an axial seam. The outer vacuum window was of 0.003-in. Mylar film which was preformed to the shape of a torus to withstand the atmospheric pressure. To prevent collapse, the bottom flange of the outer window was anchored to the base plate of the scattering assembly, the body of the target being supported from above. Thus, no massive portion of the target was in the vicinity of either the incident or the scattered beam.

The diameter and position of the target with respect to the desired geometrical scattering center were measured with a traveling telescope while the target was full of liquid hydrogen. The target center coincided with the geometrical scattering center within 0.01 in.

D. Counters and Electronics

1. Counter Telescopes

Three different gamma-ray telescopes were used in this experiment. They will be referred to as the "3 in.," the "8 in.," and the "6 in." telescopes (see Fig. 2). Each consisted of a scintillation guard counter No. 6 in anticoincidence, two scintillation counters Nos. 3 and 4, and a water Čerenkov counter. All scintillation counters were made of plastic scintillator and were mounted on RCA 6810-A photomultiplier tubes. A lead converter was inserted between Nos. 6 and 3. The No. 3 and No. 4 counters were large enough to count

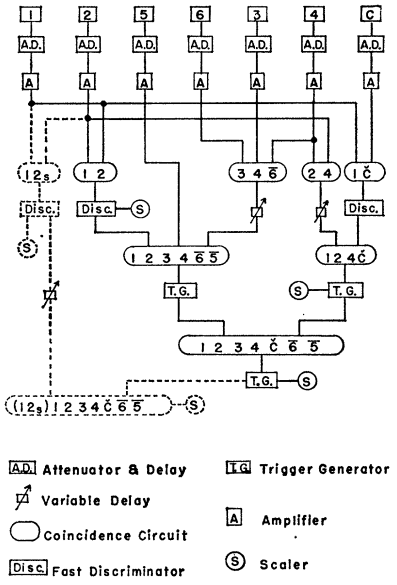

FIG. 6. Block diagram of electronics for one counter telescope.

the conversion electrons from any gamma ray originating in the illuminated target volume and converting in the lead. The size of No. 6 was such as to count any particle that passed through the other three counters.

The "3-in." telescope, used for measuring the angular distribution of the gamma rays at 31 Mev, had an angular acceptance of approximately 10°. The converter was 2 in. high by 1 in. by 0.20 in. The Čerenkov counter was a 3-in. i.d. cylinder of polished aluminum, filled with water, viewed by an RCA 7246 photomultiplier.

The "8-in." telescope, used for the total cross-section measurement at 31 Mev, had a 2-in. diameter converter 0.060 in. thick. To provide an adequate path length in the water for electrons from gamma rays near the limits of the angular acceptance, the Čerenkov counter was made in a "conical" shape (see Fig. 2). For uniformity of light collection, the inner surface was painted with white Krylon enamel. A round-faced RCA 7246 tube was also used to improve the light collection. Despite these precautions, this Čerenkov counter had a slight loss of efficiency at its extreme edges, but this loss amounted to only 2.3%.

The "6-in." telescope was designed as a replacement for the "8-in." telescope, and was used for some of the 31-Mev and all of the 20-Mev measurements. Its converter was $1\frac{3}{4}$ in. in diameter and 0.050 in. thick. The Čerenkov counter was a 6-in. diameter Mu-metal cylinder, painted white, mounted on an RCA 7046 5-in. photomultiplier. This arrangement proved to be fully efficient for all angles. The loss in counting rate due to the smaller converter was compensated by the decreased background due to the smaller counters and to the lower gain required in the Čerenkov counter.

The scattering telescopes were calibrated for electrons by setting them in the incident beam and using the 110-Mev contamination electrons, which are close to minimum ionization.

2. *Electronics*

The requirements for an event to be recorded were $1+2+\bar{5}+3+4+\bar{6}+\check{C}$. (The bar indicates anticoincidence.) The No. $\bar{5}$ anticoincidence counter, placed behind the target, helped to reduce the background.

The electronic arrangement for one telescope is illustrated in a simplified block form in Fig. 6. The signals from the photomultipliers were shaped by shorted clipping lines at the input of the amplifiers. The lengths of these were 2 and 3 ft for coincidence and anticoincidence inputs, respectively. The resolving time of a typical first stage coincidence was 8 nsec (full width, half-maximum). Because the coincidences at succeeding stages were made with shaped pulses from trigger circuits, the resolving times were about five times as great. Therefore, to reduce randoms between the incident-beam telescope and the scattering telescopes, the photomultiplier outputs were split to make the fast coincidences $(1+\check{C})$ and $(2+4)$.

The simplified transistorized coincidence circuit developed at Chicago by Miller[8] was used throughout. An important characteristic of this circuit is that the output pulse height is well governed by the smaller of the two input pulses. This makes it possible to set the discriminator after the circuit to reject small pulses without losing the fast resolving time inherent in this coincidence circuit.

A fast transistorized discriminator-scaler,[9] modified by removing the input amplifier and adding a one-stage limiting amplifier to the output, was used after the coincidence circuits where counting rates were high. Transistorized univibrator trigger circuits were used after circuits with low counting rates. These circuits provide a positive scaler output pulse in addition to a shaped pulse for driving succeeding coincidence stages.

IV. DATA AND CORRECTIONS

The corrections to the data at 31 Mev can be separated into those which are common to all measurements, and those which are dependent on the telescope in use. The data at 20 Mev is also listed in this way, but the separation is unnecessary since only one telescope was used. The common corrections are listed in Table I, telescope-dependent ones in Table II.

The correction listed as "slow mesons $\leq$10.5 Mev" requires some explanation. As is known, every π^- meson that stops in hydrogen gives rise, on the average, to 1.6 gamma rays (Panofsky gammas). Thus if approximately 0.1% of the incident pions were to stop

[8] R. H. Miller, Rev. Sci. Instr. **30**, 395 (1959).
[9] M. Gettner and W. Selove, Rev. Sci. Instr. **30**, 942 (1959).

in the target, as many gammas would be produced from this source as from the reaction of interest.

The correction was made by rejecting or subtracting all gamma rays in coincidence with low-energy pions in the incident beam, and subtracting the number of low-energy pions recorded from the number of incident-beam monitor counts.

The circuit shown in dashed lines in Fig. 6 was used to count these gamma rays. It was possible to distinguish the low-energy pions by their pulse height in the incident telescope counters. A 10-Mev pion has just enough energy to traverse the thickest part of the hydrogen target. Such pions have a dE/dx which is 2.1 times that of 30-Mev pions; 1.7 times that of 20-Mev pions. To calibrate this circuit, the incident pion beam was degraded to 10.5 Mev with a copper absorber. The discriminator was set to count these pions with $(99\pm1)\%$ efficiency. In operation, at 31 Mev this circuit was triggered by $(0.60\pm0.08)\%$ of the pions counting in the (1+2) monitor circuit; at 20 Mev the fraction was $(1.9\pm0.5)\%$.

At 31 Mev, the measurement of the slow pion gammas was made with the "6-in." telescope at the end of the run. $(8\pm3)\%$ of the observed events were due to slow pions. These events were subtracted, the statistical uncertainty being obtained from the sum of the two rates in the usual way.

At 20 Mev the slow mesons accounted for $(39\pm3)\%$ of the observed effect. The statistical subtraction of such a large fraction significantly increases the uncertainty. Therefore, the circuit was used as indicated in the figure to count simultaneously the gammas produced from all incident pions and from just the slow pions. These two measurements were completely correlated, so the subtraction could be done directly, the statistical uncertainty being derived from the difference of the two rates.

A sizeable amount of data at 20 Mev was taken without this circuit. This data was corrected by statistically subtracting (as at 31 Mev) the number of events due to the slow pions.

TABLE I. Common corrections and uncertainties.

Type of correction	31.0 Mev	20.7 Mev
A. Corrections to the incident beams (%).		
Electron contamination	+5.0 ±0.9	+4.1 ±0.5
Muon contamination	+4.2 ±1.0	+4.9 ±0.9
Total contamination	+9.2 ±1.4	+9.0 ±1.1
Slow pions ($\leq$10.5 Mev)	+0.60±0.08	+1.85±0.50
Room background	+0.55±0.15	+0.57±0.11
Fraction of beam missing target	+0.00±0.5	+0.00±0.5
B. Corrections common to all data at both energies (%).		
Dalitz pairs	+0.7 ±0.1	
Gamma-ray absorption in hydrogen	+0.16±0.05	
Gamma-ray absorption in Mylar target walls	+0.03±0.01	
Gamma-ray absorption in No. 6 counter	+0.05±0.01	
Absolute gamma cross section	+0.00±1.6	

TABLE II. Telescope-dependent corrections and uncertainties (%).

Type of correction	Telescope 3 in.	8 in.	6 in.
No-converter efficiency	−1.5±0.5	−2.7±0.7	−2.5±0.7
3+4 efficiency	···	+0.9±0.5	+2.6±1.5
No. 6 anticoincidence randoms	···	+1.5±0.4	+1.5±0.4
No. 5 anticoincidence randoms	···	+0.4±0.4	0.4±0.4
Angular acceptance function	+0.0±2.5	0.0±2.6	0.0±2.5
$F(k)$ approximation	···	0.0±0.6	0.0±0.6

The source of the low energy pions in the beam was not fully investigated. However, the number of slow pions is certainly increased many times by the presence of the polyethylene degrader at 20 Mev.

From the particular gain settings chosen it was calculated that any gamma ray that converted in the last third of the No. 6 anticoincidence crystal, in the front half of the No. 3 counter, or in any of the wrappings between, was recorded as a real event. This correction is listed as "no-converter efficiency" in Table II.

The angular acceptance-efficiency function of each telescope was computed numerically on the IBM 650 computer. Because of practical limitations on computing time, the regions of integration of the variables were divided into six intervals and the integration was approximated by Simpson's rule. To test the error introduced in this way, the regions were divided into 30 intervals for a few sample points. The weighted mean correction from this test is included in the error. The uncertainty in the position of the converter and in the beam intensity distribution also contribute to the error assigned to the angular acceptance function.

The effect of the competing reaction, $\pi^-+p\rightarrow\gamma+n$ on the counting rate was calculated from the inverse pion production cross section, using the principle of detailed balancing

$$d\sigma(\pi^-+p\rightarrow\gamma+n)=(P_\gamma^2/P_\pi^2)2Rd\sigma(\gamma+p\rightarrow\pi^++n)$$

where

$$R=d\sigma(\gamma+n\rightarrow p+\pi^-)/d\sigma(\gamma+p\rightarrow n+\pi^+)$$

TABLE III. Number of counts per 10^6 incident pions and the expected number calculated from the least-squares fit. The corrections in Tables I and II have been applied.

Telescope	θ	Counts from radiative capture	Corrected experimental	Calculated
		31 Mev		
6 in.	90.0°	0.54±0.09	8.03±0.76	8.23
8 in.	83.0°	0.79±0.14	12.82±0.86	12.65
3 in.	33.2°	0.44±0.08	4.92±0.67	5.05
3 in.	61.8°	0.50±0.08	6.32±0.71	5.96
3 in.	90.0°	0.49±0.08	6.85±0.81	6.86
3 in.	108.7°	0.49±0.08	7.46±0.80	7.77
3 in.	127.6°	0.45±0.08	7.95±0.92	8.53
3 in.	143.9°	0.40±0.08	9.80±1.02	9.05
		20.7 Mev		
6 in.	90.0°	0.56±0.09	6.76±0.47	···

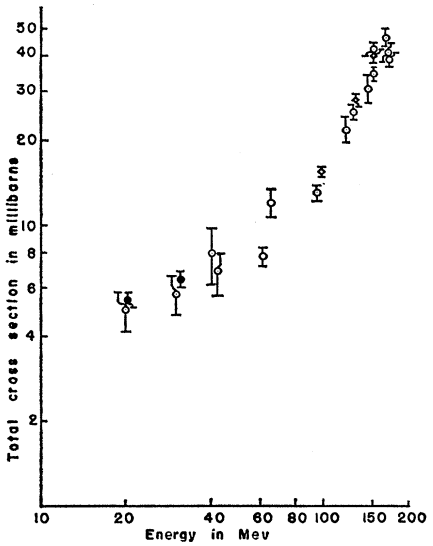

FIG. 7. Total cross sections for the charge exchange reaction below 170 Mev. References in order of increasing energy are: Spry[1]; this paper; Spry[1]; this paper; Tinlot and Roberts[3]; Spry[1]; York *et al.*[11]; Bodansky *et al.*[12]; York *et al.*[11]; Edwards *et al.*[13]; Anderson *et al.*[14]; Garwin *et al.*[15]; Kruse and Arnold[16]; Anderson *et al.*[14]; Kernan[17]; Ashkin *et al.*[18]; York *et al.*[11]; Anderson and Glicksman[19]; Fermi *et al.*[20]; and Ashkin *et al.*[21]

and is determined from the ratio of negative and positive photoproduction from deuterium. P_γ and P_π are the center-of-mass momenta of the gamma ray and pion.

The number of counts per million incident pions (assuming 100% efficiency) in each telescope was calculated from the angular distribution of the gamma rays and the angular acceptance functions. These counts were subtracted from the experimentally determined counting rates (after the corrections listed in Tables I and II were made). The numbers of counts from the radiative capture are listed in Table III.

V. RESULTS AND ANALYSIS

A. Legendre Polynomial Expansion

A least-squares fit of the data to Eq. (10) was done with the IBM 650 computer using a modification of the procedure described in reference 5. As mentioned earlier, the gamma-ray conversion efficiency was approximated by

$$F(k)=t(\theta,\phi)\ p(1+r\ \ln k). \tag{6}$$

For the "6-in." and "8-in." telescopes this approximation deviated from the actual $F(k)$ by less than 0.6%. For the "3-in." telescope, the rather thick converter used meant that the shower processes were important. Wilson's results[10] show that Eq. (6) is still a good approximation, but the value of p is more difficult to calculate. Also, the Čerenkov counter was somewhat small for the size of the converter. Therefore, $I_F(\theta)$ was considered to be also a function of p for this telescope and p was included as a parameter to be normalized by the data from the "6-in." and "8-in." telescopes. The dependence of the output on the value of r was tested by inserting different values over the region of uncertainty. A calculation was also made assuming that the Čerenkov counters had a low-energy cutoff of 10 Mev. The effects found by these checks are included in the stated errors.

The result of the analysis of the 31-Mev data was:

$$d\sigma/d\Omega=(1.00\pm0.02)$$
$$\times[(0.51\pm0.04)-(0.61\pm0.11)P_1(\cos\theta)$$
$$+(0.12\pm0.36)P_2(\cos\theta)]\text{mb/sr},$$
$$\sigma_{\text{tot}(31\text{ Mev})}=4\pi A_0=6.5\pm0.5\text{ mb}.$$

The error matrix in units of $(\text{mb/sr})^2$ is:

	A_0	A_1	A_2
A_0	0.001213	−0.001954	0.007562
A_1	···	0.010780	−0.019158
A_2	···	···	0.125196

$$\chi^2=1.49$$

At 20.7 Mev, where only the "total cross section" was measured, the data was analyzed for A_0, inserting as constants A_1 and A_2 calculated from the above 31-Mev values, assuming the usual dependencies. The effect of the choice of the higher terms was tested by repeating the analysis, letting A_1 and A_2 assume values ranging from zero to the values at 31 Mev. The maximum change in A_0 was 2.5% for $A_1=A_2=0$. Therefore, as expected, the contribution of these terms is not important. An error of 2% was assigned for the uncertainty in A_0 from this source.

$$A_0(20.7\text{ Mev})=0.431\pm0.032\text{ mb/sr},$$
$$\sigma_{\text{tot}(20.7\text{ Mev})}=4\pi A_0=5.42\pm0.40\text{ mb}.$$

The measured total cross sections from the literature[1,3,11–21] below 170 Mev are shown in Fig. 7.

B. Phase Shift Analysis

The data was also analyzed in terms of phase shifts, expressing the A_i as functions of the s and p phase

[10] R. R. Wilson, Phys. Rev. **86**, 261 (1952).

[11] G. M. York, W. J. Kernan, and E. L. Garwin, Phys. Rev. **119**, 1096 (1960).

[12] D. Bodansky, A. M. Sachs, and J. Steinberger, Phys. Rev. **93**, 1367 (1954).

[13] D. N. Edwards, S. G. F. Frank, and J. R. Holt, Proc. Phys. Soc. (London) **73**, 856 (1959).

[14] H. L. Anderson, E. Fermi, R. Martin, and D. E. Nagle, Phys. Rev. **91**, 155 (1953).

[15] E. Garwin, W. J. Kernan, C. O. Kim, and C. M. York, Phys. Rev. **115**, 1295 (1959).

[16] U. E. Kruse and R. C. Arnold, Phys. Rev. **116**, 1008 (1959).

[17] W. J. Kernan, Phys. Rev. **119**, 1092 (1960).

[18] J. Ashkin, J. Blaser, F. Feiner, and M. O. Stern, Phys. Rev. **101**, 1149 (1956).

[19] H. L. Anderson and M. Glicksman, Phys. Rev. **100**, 268 (1955).

[20] E. Fermi, M. Glicksman, R. Martin, and D. E. Nagle, Phys. Rev. **92**, 161 (1953).

[21] J. Ashkin, J. Blaser, F. Feiner, and M. O. Stern, Phys. Rev. **105**, 724 (1957).

shifts. The charge exchange data alone is not sufficient to determine all six s and p wave phase shifts. Therefore, the set of $\pi^+ + p \rightarrow \pi^+ + p$ data, referred to as combination D in reference 5, was used to provide the $T=\frac{3}{2}$ phase shifts. This data has been re-analyzed using the new Coulomb correction provided by H. Schnitzer.[22] This extends the Coulomb corrections of Van Hove[23] and of Schnitzer and Salzman[24] by the addition of a so-called "inner Coulomb correction" as suggested by Hamilton and Woolcock.[25]

$$S \text{ waves} \quad \alpha\{\epsilon+\ln 2\rho_0-\mathrm{Ci}(2\rho_0)\cos 2\alpha_i{}^N + \mathrm{Si}(2\rho_0)\sin 2\alpha_i{}^N-\rho_0{}^2\},$$

$$P \text{ waves} \quad \alpha\Big\{\epsilon+\ln 2\rho_0-1-\mathrm{Ci}(2\rho_0)\cos 2\alpha_{ij}{}^N + \mathrm{Si}(2\rho_0)\sin 2\alpha_{ij}{}^N-\frac{1}{2\rho_0{}^2}[1-\cos^2(\rho_0+\alpha_{ij}{}^N)] + \frac{\sin^2(\rho_0+\alpha_{ij})}{\rho_0}-\frac{\rho_0{}^4}{15}\Big\}, \quad (11)$$

where ϵ is Euler's constant, $\rho_0=kr_0$,

$$\mathrm{Ci}(x)=-\int_x^\infty \frac{\cos x}{x}dx,$$

$$\mathrm{Si}(x)=-\int_x^\infty \frac{\sin x}{x}dx,$$

and $\alpha=e^2/\hbar v$, where v is the relative velocity of the pion and nucleon. Fig. 8 shows that the inclusion of the inner Coulomb correction term makes the correction

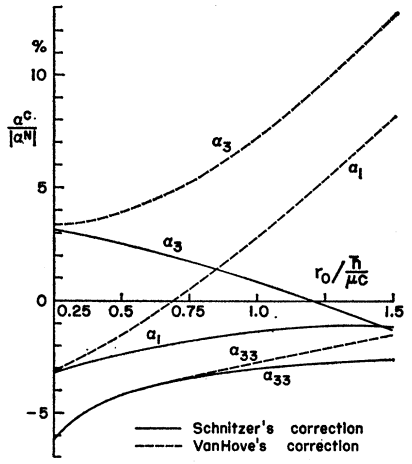

FIG. 8. Dependence of Coulomb corrections on the choice of r_0.

[22] H. J. Schnitzer (private communication).
[23] L. Van Hove, Phys. Rev. 88, 1358 (1952).
[24] H. J. Schnitzer and G. Salzman (private communication).
[25] J. Hamilton and W. S. Woolcock, Phys. Rev. 118, 291 (1960).

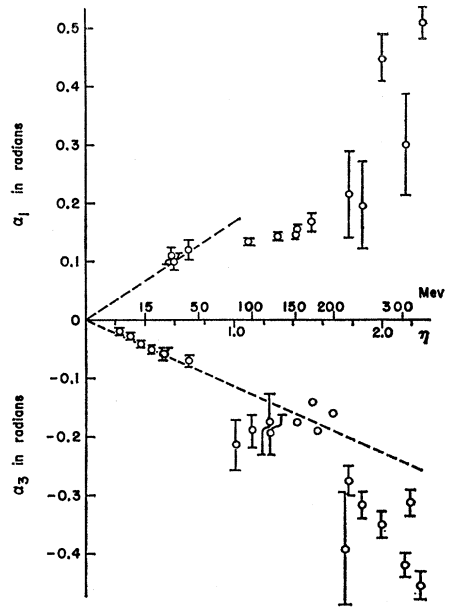

FIG. 9. Plot of α_1 and α_3 against η for available data.

less dependent on the choice of r_0. The following momentum dependencies were assumed:

$$\alpha_{31}{}^N=a_{31}\eta^3,$$

$$\alpha_3{}^N=a_3\eta,$$

$$\tan\alpha_{33}{}^N=\tfrac{4}{3}\eta^3\frac{f^2}{\omega^*(1-\omega^*/\omega_0{}^*)}.$$

The results are:

$$a_{31}=-0.041\pm0.004,$$
$$a_3=-0.107\pm0.003,$$
$$f^2=+0.088\pm0.001.$$

These results differ from those of the previous papers[5,6] only in the case of a_3 which is 7% smaller.

The 31-Mev data then yields the following set of phase shifts:

$$\alpha_1{}^N=0.100\pm0.015=+(0.17\pm0.03)\eta,$$
$$\alpha_{11}{}^N=0.010\pm0.060=+(0.05\pm0.33)\eta^3,$$
$$\alpha_{13}{}^N=-0.030\pm0.015=-(0.14\pm0.07)\eta^3.$$

Assuming that the phase shifts obey the indicated momentum dependencies, at least over the 20–30 Mev region, the 31-Mev phase shifts were used to calculate the 20.7-Mev experimental results. The agreement was within half a standard deviation, showing that the data are self-consistent.

A quantity of interest is the value of (a_1-a_3), where a_i is defined by

$$\alpha_i=a_i\eta+b_i\eta^3+\cdots. \quad (12)$$

This value can be obtained from the threshold pion photoproduction data and the Panofsky ratio. The current prediction[25] for this value is $(a_1-a_3)=0.245 \pm 0.010$. If we assume a linear momentum dependence for α_1 and α_3, i.e., take only the first term in (12), the 31-Mev data yields a value $(a_1-a_3)=0.278\pm 0.026$.

At 20.7 Mev the expression

$$\sigma_{\text{tot}}=(8\pi\lambda^2/9)(\alpha_1-\alpha_3)^2 +2(\alpha_{33}-\alpha_3)^2+(\alpha_{31}-\alpha_{11})^2 \quad (13)$$

was solved for $(\alpha_1-\alpha_3)$, assuming that the other phase shifts obeyed the momentum dependencies given above. The result was

$$(\alpha_1-\alpha_3)/\eta=0.272\pm 0.025.$$

These values are in fair agreement with the prediction from the other low-energy data.

However, in order to make a proper comparison of these results, we must know the actual momentum dependence of the phase shifts from 0 to 30 Mev. Theoretically Cini *et al.*[26] have shown from crossing symmetry and Hamilton and Woolcock[25] from the finite momentum transfer dispersion relations of Chew, Low, Goldberger, and Nambu[27] that $(\alpha_1-\alpha_3)$ is not linear in η and that the value of (a_1-a_3) should be smaller than that obtained by a linear extrapolation.

In Fig. 9, a plot of α_1 and α_3 vs η is shown for a wide range of available data. The straight lines shown are those obtained from the combination D data of reference 5. A small nonlinear dependence may well be indicated by the data in Fig. 9. Thus, there is some indication on both theoretical and experimental grounds that the behavior of $(\alpha_1-\alpha_3)$ is slightly nonlinear in the low-energy region. This would tend to improve the already reasonable agreement between (a_1-a_3) obtained from the linear extrapolation to zero energy of the scattering results reported in this paper, and the predictions from the other low-energy pion phenomena.

[26] M. Cini, R. Gatto, E. L. Goldwasser, and M. A. Ruderman, Nuovo cimento **10**, 242 (1958).
[27] G. F. Chew, M. L. Goldberger, F. E. Low, and Y. Nambu, Phys. Rev. **106**, 1337 (1957).

ACKNOWLEDGMENTS

The authors wish to express their gratitude to Professor S. W. Barnes for his advice and encouragement throughout this work. Many others at this laboratory have made contributions. In particular, we wish to thank Alex Wieber for his help in assembling and aligning the apparatus; Fred Palmer and the operating crew for the many hours of cyclotron operation; and the staff of the mechanical and electronics shops for their help in constructing and maintaining the equipment. One of us (K. Miyake) is indebted to the Fulbright Commission for a travel grant.

PHYSICAL REVIEW VOLUME 126, NUMBER 6 JUNE 15, 1962

Investigation of Light Fragmentation Products and Peculiarities of Nuclear Fission at High Energies of Incident Particles

P. A. Goritchev, V. F. Darovskikh, O. V. Lozhkin, A. I. Obukhov, N. A. Perfilov, and U. P. Jakovlev
Radium Institute, Academy of Sciences, Leningrad, U.S.S.R.

(Received November 2, 1961)

Nuclear emulsions were used to study the charge spectrum of fragments and the multiplicity of fragment production in disintegrations of Ag and Br nuclei caused by incident 9-Bev protons. The paper contains some new results of investigation of fission of Pb, Bi, and U with 660-Mev protons.

I. INTRODUCTION

THE paper contains some new results of investigation of fission and fragmentation in nuclear emulsions. The advantages of observing individual disintegrations were used to study various correlations in fragmentation and fission processes to obtain additional data necessary to understand the mechanism of these processes.

The following features of fragmentation were investigated: 1. The dependence of the charge spectrum of fragments (with $3\leq Z\leq 9$) on the amount of energy transferred to the nucleus by the incident proton, and on the direction of emission of fragments relative to the incident proton direction. 2. Correlation of charges, energies, and angles of fragment emission in case of multiple fragment production.

The following features of fission of U, Bi, and Pb nuclei were studied: 1. The dependence of mean combined fragment range on the range ratio of light and heavy fission fragments. 2. The fission yields for Pb and Bi fission in relation to the range ratio. 3. The U and Bi fission anisotropy at the incident proton energy of 660 Mev.

The superfine grained P-9(S) emulsions were irradiated at Dubna with proton beams from the synchrotron (9 Bev) and synchrotron (660 Mev). The methods used are similar to those described in previous